



Aalborg Universitet

AALBORG UNIVERSITY
DENMARK

A collagen-based layered chronic wound biofilm model for testing antimicrobial wound products

Thaarup, Ida C.; Lichtenberg, Mads; Nørgaard, Kim T.H.; Xu, Yijuan; Lorenzen, Jan; Thomsen, Trine R.; Bjarnsholt, Thomas

Published in:
Wound Repair and Regeneration

DOI (link to publication from Publisher):
[10.1111/wrr.13087](https://doi.org/10.1111/wrr.13087)

Creative Commons License
CC BY-NC-ND 4.0

Publication date:
2023

Document Version
Publisher's PDF, also known as Version of record

[Link to publication from Aalborg University](#)

Citation for published version (APA):
Thaarup, I. C., Lichtenberg, M., Nørgaard, K. T. H., Xu, Y., Lorenzen, J., Thomsen, T. R., & Bjarnsholt, T. (2023). A collagen-based layered chronic wound biofilm model for testing antimicrobial wound products. *Wound Repair and Regeneration*, 31(4), 500-515. <https://doi.org/10.1111/wrr.13087>

General rights




Copyright and moral rights for the publications made accessible in the public portal are retained by the authors and/or other copyright owners and it is a condition of accessing publications that users recognise and abide by the legal requirements associated with these rights.

- Users may download and print one copy of any publication from the public portal for the purpose of private study or research.
- You may not further distribute the material or use it for any profit-making activity or commercial gain
- You may freely distribute the URL identifying the publication in the public portal -

Take down policy

If you believe that this document breaches copyright please contact us at vbn@aub.aau.dk providing details, and we will remove access to the work immediately and investigate your claim.

A collagen-based layered chronic wound biofilm model for testing antimicrobial wound products

Ida C. Thaarup PhD¹  | Mads Lichtenberg PhD¹  | Kim T. H. Nørgaard MSc² |
Yijuan Xu PhD^{2,3} | Jan Lorenzen PhD³ | Trine R. Thomsen PhD^{2,3}  |
Thomas Bjarnsholt PhD^{1,4}

¹Department of Immunology and Microbiology, Faculty of Health Sciences, University of Copenhagen, Copenhagen, Denmark

²Center for Microbial Communities, Aalborg University, Aalborg East, Denmark

³Environmental Technology, Danish Technology Institute, Aarhus, Denmark

⁴Department of Clinical Microbiology, Copenhagen University Hospital, Copenhagen, Denmark

Correspondence

Ida C. Thaarup, Department of Immunology and Microbiology, Faculty of Health Sciences, University of Copenhagen, Copenhagen, Denmark.

Email: icthaarup@sund.ku.dk

Funding information

Magle Chemoswed AB; Novo Nordisk Fonden, Grant/Award Numbers: NNF19OC0054390, NNF19OC0056411

Abstract

A new in vitro chronic wound biofilm model was recently published, which provided a layered scaffold simulating mammalian tissue composition on which topical wound care products could be tested. In this paper, we updated the model even further to mimic the dynamic influx of nutrients from below as is the case in a chronic wound. The modified in vitro model was created using collagen instead of agar as the main matrix component and contained both *Staphylococcus aureus* and *Pseudomonas aeruginosa*. The model was cast in transwell inserts and then placed in wound simulating media, which allowed for an exchange of nutrients and waste products across a filter. Three potential wound care products and chlorhexidine digluconate 2% solution as a positive control were used to evaluate the model. The tested products were composed of hydrogels made from completely biodegradable starch microspheres carrying different active compounds. The compounds were applied topically and left for 2–4 days. Profiles of oxygen concentration and pH were measured to assess the effect of treatments on bacterial activity. Confocal microscope images were obtained of the models to visualise the existence of microcolonies. Results showed that the modified in vitro model maintained a stable number of the two bacterial species over 6 days. In untreated models, steep oxygen gradients developed and pH increased to >8.0. Hydrogels containing active compounds alleviated the high oxygen consumption and decreased pH drastically. Moreover, all three hydrogels reduced the colony forming units significantly and to a larger extent than the chlorhexidine control treatment. Overall, the modified model expressed several characteristics similar to in vivo chronic wounds.

KEYWORDS

biofilm, chronic wounds, in vitro, microenvironment

Abbreviations: CFU, colony forming unit; CHX, chlorhexidine gluconate; CWB, chronic wound biofilm; EPS, extracellular polymeric substances; mCWB, modified chronic wound biofilm; ON, overnight; PBS, phosphate-buffered saline; WGA, wheat germ agglutinin; WSM, wound simulating medium.

This is an open access article under the terms of the [Creative Commons Attribution-NonCommercial-NoDerivs](https://creativecommons.org/licenses/by-nc-nd/4.0/) License, which permits use and distribution in any medium, provided the original work is properly cited, the use is non-commercial and no modifications or adaptations are made.

© 2023 The Authors. *Wound Repair and Regeneration* published by Wiley Periodicals LLC on behalf of The Wound Healing Society.

1 | INTRODUCTION

The rising incidence of diabetes, blood pressure diseases, overweight and a population with an increased lifespan are some of the reasons why chronic wounds, particularly on lower limbs, are increasing every year.¹ To date, one of the most reliable treatments used by physicians is sharp debridement and removal of dead and infected tissue. However, since debridement rarely removes every single microbe, any remaining bacteria may repopulate the wound.² For this reason, supporting topical treatments are requested by the physicians, although these are often lacking in efficiency when used in the clinic.³

For developing new wound care treatments, good in vitro models are a necessity. The more realistic the model is, the higher the likelihood that data obtained from the lab-scale in vitro model can be translated to in vivo conditions and the treatment can prove successful in practice.

We have previously published some ideas about the 'perfect' in vitro biofilm infected chronic wound model.⁴ In line with these thoughts, we wanted our new model to:

- Contain Wound Simulating Medium (WSM)
- Be based on a matrix of suitable mammalian material
- Have nutrients continuously added
- Be able to contain several selected microbial species
- Express 3D gradients of nutrients, oxygen and pH
- Be devoid of shear flow
- Be devoid of non-mammalian components in the matrix or the media
- Not be grown on a solid surface

The modified model in the present study was based on the layered chronic wound biofilm model (CWB) recently published by Chen et al.,⁵ which contained both *Staphylococcus aureus* and *Pseudomonas aeruginosa*. However, we made some significant changes according to the abovementioned criteria. First, the matrix material was changed from agar to collagen, and thus from a plant-derived to a mammalian, human-relevant material. We hypothesized that changing the matrix could affect antimicrobial tolerances. Second, the models were cast in transwell inserts. This allowed for an exchange of nutrients and waste products from the bottom without introducing shear flow. It was hypothesized that it would allow the model to sustain growth for a significantly longer period and maintain steady state in terms of bacterial numbers and species-to-species ratio. Third, the physiological salt water in the original model was replaced with phosphate-buffered saline (PBS). It was conjectured that the buffered system would provide a more realistic environment. Chronic wounds are often characterised by (i) an excess of nutrients where damaged tissue is assumed to release a range of nutrients,⁶ (ii) an alkaline pH that is thought to be partially due to bacterial activity, as several species are converting nitrous compounds by ammonification leading to a net pH increase⁷ and (iii) predominantly hypoxic/anoxic conditions.⁸ The oxygen depletion within chronic wounds⁹ is likely a result of the concerted oxygen

consumption of both bacteria and immune cells that consume O₂ for the production of the superoxide anion (O₂⁻) used in their respiratory burst.¹⁰⁻¹² Finally, the original CWB model was grown at room temperature, while the modified model instead was grown at 33°C, to more accurately reflect the average temperature found in the wound bed of chronic ulcers.¹³

Three new hydrogels made from degradable starch microspheres carrying different active compounds were tested for their antimicrobial effect on the modified in vitro model. A 2% chlorhexidine digluconate solution (CHX) was used as a control. This compound has previously been shown to be effective against both *S. aureus* and *P. aeruginosa* and is currently used as a topical solution for infected wounds.¹⁴ Since the newest recommendations for wound care advise against the use of topical antibiotics, we decided not to test antibiotics in the modified in vitro model.¹⁵ All treatments were tested in the original CWB model for comparison.

The motivation for making this new, modified in vitro model was to create a wound-like microenvironment, in which novel topical products could be tested under in vivo-like conditions. We wanted to grow wound-relevant pathogens while emulating several environmental factors, such as pH, oxygen and temperature levels as well as a continuous supply of nutrients, as we believe such factors to have a large impact on potential treatments. Finally, we wanted the model to be economically viable using readily sourced materials, and be easy to replicate, giving the opportunity for semi-high throughput screenings of new wound treatments.

2 | METHODS

2.1 | The layered CWB model

The layered chronic wound models produced for the present study were made exactly as described previously, by Chen et al.⁵ The only change in this study was the incubation temperature which was increased from room temperature to 33°C.

2.2 | The modified layered chronic wound biofilm model (mCWB)

Similar to the original, the modified model created for the present study consisted of a dermis-like layer on top of a subcutaneous fat-like layer.

The dermis-like layer consisted of 2% peptone water (Oxoid) (w/v), 50% cattle serum (Sigma) (v/v), 5% laked horse blood (SSI Diagnostica) (v/v), 10% 10× PBS (v/v) and 21% distilled water (v/v). Alpha-amylase (A6255, Sigma-Aldrich) was added to a final concentration of 140 U/L. Highly concentrated rat tail tendon collagen (type 1) (Corning Inc.) was added to a final concentration of 2 mg/mL. This was neutralised with NaOH by adding 0.023 μL of a 1 N NaOH solution times the added collagen volume in μL. This solution was prepared on ice and kept on ice until use.

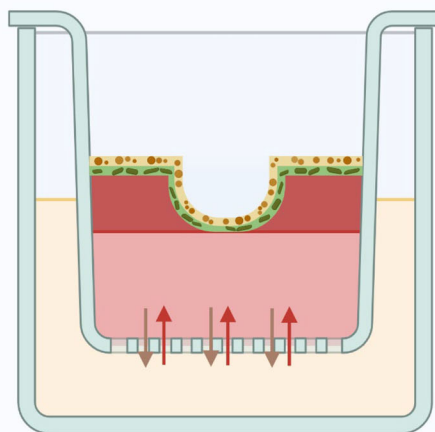
The Modified Layered Chronic Wound Biofilm Model (mCWB)

Dermis-like layer

- Serum
- Laked whole blood
- Peptone meat digest
- Phosphate buffered saline
- Collagen
- α -amylase

Fat-like layer

- Serum
- Laked whole blood
- Peptone meat digest
- Phosphate buffered saline
- Collagen
- α -amylase
- Fat



Microorganisms

- *S. aureus* added on top
- *P. aeruginosa* added below

Incubation temperature

- 33°C

Wound simulating medium

- Serum
- Saline buffered peptone

Design

Cast in transwell inserts to allow continuous exchange of nutrients and waste products

FIGURE 1 Schematic drawing of the modified layered chronic wound biofilm model.

The subcutaneous fat-like layer was prepared on ice and made of 2% peptone water (w/v), 10% pig fat (w/v), 20% cattle serum (v/v), 2% laked horse blood (v/v), 10% 10 \times PBS (v/v) and 56% distilled water (v/v). Alpha-amylase was added to a final concentration of 140 U/L. A final collagen concentration of 2 mg/mL neutralised with NaOH was obtained, as described above. The transwell inserts (0.4 μ m pore size) (ThermoFisher Scientific) were pre-heated on a heating block set to 65°C together with the pig fat, which was melted before being added separately into each insert. Afterwards, the transwell inserts were slowly cooled down to room temperature. The rest of the subcutaneous fat-like solution was then removed from the ice, left at room temperature for 5 min before being added to the transwell inserts and mixed with the melted pig fat.

The subcutaneous fat-like layer was left at 37°C to polymerise for 1 h. Small round silicone moulds of a 6 mm diameter were placed on the polymerised subcutaneous fat-like layer before casting the dermis-like layer on top creating the signature 'void' presented in Chen et al.⁵ After the addition of the dermis-like layer, the model was left for another hour at 37°C to polymerise where after the moulds were removed, and excess liquid aspirated.

Overnight (ON) cultures of GFP-tagged *S. aureus* (strain RN4220) and mCherry-tagged *P. aeruginosa* (strain PAO1) were grown in LB medium the day before making the models. Both strains originate from human infections as PAO1 was originally isolated from a wound while RN4220 was originally isolated from a corneal ulcer. An estimate of 25–100 colony forming units (CFU) of *P. aeruginosa* were added to the dermis-like solution and added to each model. After 30 min at 37°C, approximately 75–200 CFU of *S. aureus* were mixed with dermis-like solution and added on top of the *P. aeruginosa* layer. After another 30 min at 37°C, each transwell insert was added to the well of a 12-well-plate. In each well, 1 mL wound simulation medium (WSM) was added, made from 50% bovine serum mixed with 50% saline buffered peptone in a 0.1% concentration. All products used in the model were purchased as sterile products.

The finished models were incubated at 33°C. The modified models were placed on a shaker set to 60 rpm and WSM was replaced every 24 h (see Figure 1 for a schematic overview of the model).

2.3 | Microscopy

Confocal microscopy imaging of the CWB model was performed as described in Chen et al.⁵ Briefly, three different stains were added to the model: Syto™9, Sytox™Orange Dead Cell Stain and wheat germ agglutinin (WGA) Alexa Fluor® 594 conjugate (Invitrogen). The model was left to incubate with the stains in darkness for 15 min, before thin vertical slices were cut with a razor blade.

For the mCWB model, fluorophore-tagged bacteria were used, making it easy to distinguish between the two species. *S. aureus* was GFP-tagged (green) while *P. aeruginosa* was mCherry-tagged (red) hence the only stain added to the modified model was Sytox™Blue Dead Cell Stain (Invitrogen). The models were wrapped in foil, snap-frozen in dry ice for 10 min, and then thin vertical slices were cut using a razor blade. This freezing step was performed to increase sectioning precision.

Sections of the models were visualised in a Zeiss LSM 880 inverted confocal laser scanning microscope (Carl Zeiss GmbH) using both a 10 \times and 63 \times oil objective and the images were subsequently processed using the IMARIS software (Bitplane AG). For overview images, a tile-scan approach was used.

2.4 | pH and oxygen measurements

Oxygen and pH measurements were performed using electrochemical microsensors. The pH microelectrode and reference electrode both had sensor tip diameters of 100 μ m (PH-100, Unisense A/S, Aarhus,

Denmark) and the oxygen microelectrode had a 25 μm diameter sensor tip (OX-25, Unisense A/S, Aarhus, Denmark). Sensors were connected to a Microsensor Multimeter (Unisense A/S) and controlled by a PC running the software Sensortrace Suite (Unisense A/S). The microsensor tips were positioned in the middle of the void of the model, and signals were recorded in vertical increments of 100 μm until a depth of 1100 μm . During measurements, models were kept at 33°C by being placed on a thermostatic heating block.

pH measurements were also performed for a sample of each treatment (see Table 1).

2.5 | Treatments

The three hydrogels (Hydrogel A, Hydrogel B and Hydrogel C) were provided by Magle Chemowed AB. They contained undisclosed active compounds in the form of various organic acids, hence their acidic pH. The hydrogels were made from solid degradable starch microspheres, containing liquid solutions of active compounds added to them, creating viscous gels. Magle Chemowed AB also provided a placebo gel made from the same material but containing 0.9% NaCl instead of an active compound. Chlorhexidine gluconate (CHX) was bought as a 20% dilution (Sigma-Aldrich) and diluted further to 2% in distilled water. Some models had nothing added to them, termed 'untreated'—not to be confused with the placebo treatment.

TABLE 1 pH of samples of the various treatments.

pH of treatments				
Placebo Hydrogel	Hydrogel A	Hydrogel B	Hydrogel C	CHX 2%
6.5	2.5	2.2	2.3	5.9

2.6 | Harvest and CFU enumeration

For CFU enumeration, the models were removed from their insert and added to 2 mL bead-beating tubes containing six ceramic beads (2.8 mm). Every tube also contained 1 mL 0.9% NaCl. The tubes were bead-beaten for 2×10 s at 6000 rpm. Dilution series were prepared with 0.9% NaCl and subsequently 10 μL spots were made on two types of selective media: Azide Agar (Sigma-Aldrich) which selects for *S. aureus* and Cetrimide Agar (Sigma-Aldrich) which selects for *P. aeruginosa*.

For the harvest of models treated with a hydrogel containing an active compound, the bead-beating tubes contained 1 mL of double-concentrated Dey-Engley broth (Sigma-Aldrich) instead of 0.9% NaCl to neutralise the effect of the hydrogels. For the models treated with CHX, the tubes contained 1 mL of Mueller-Hinton broth supplemented with 3% Tween 80 and 0.3% Lecithin, which successfully neutralised the CHX treatment as suggested by Zamany.¹⁶ The remainder of the steps were identical to the ones for non-treated models.

The neutralising effect of double-concentrated Dey-Engley broth against the three hydrogels was tested and confirmed beforehand, as was the neutralising effect of the Mueller-Hinton broth supplemented with Tween 80 and Lecithin against CHX (data not shown).

2.7 | Experimental setup

Following model assembly, measurements of O_2 concentration and pH, microscopy and CFU enumerations were performed after 0, 2, 4 and 6 days of incubation (see Figure 2 for experimental timeline). Immediately after casting the first models, pH and oxygen measurements were performed to establish a baseline in the model, before the bacteria were able to affect their environment. All models were then left at 33°C for 2 days, allowing the microbes to proliferate.

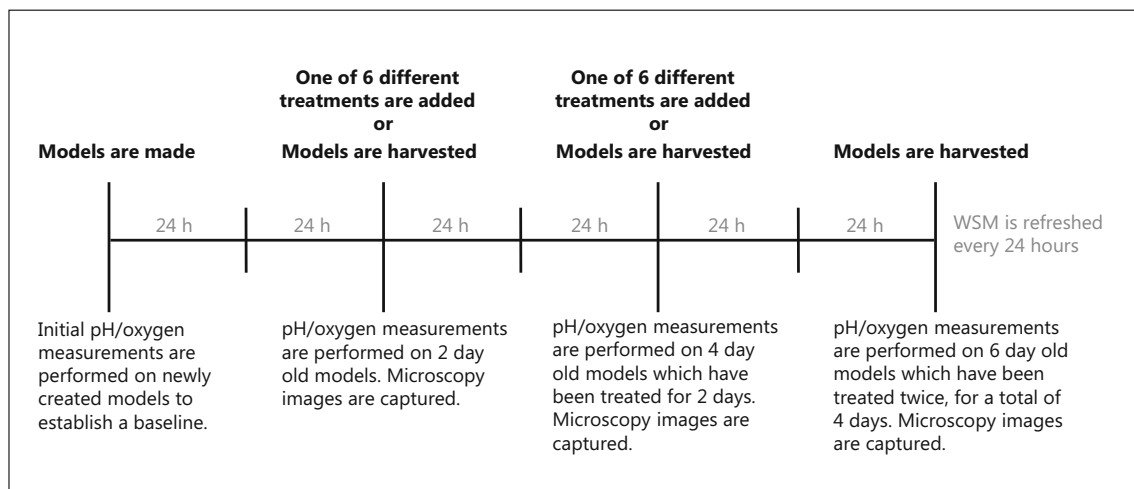


FIGURE 2 Timeline of the experimental setup of the mCWB. The experimental setup for the original CWB was similar, with the exception that no WSM was refreshed every 24 h.

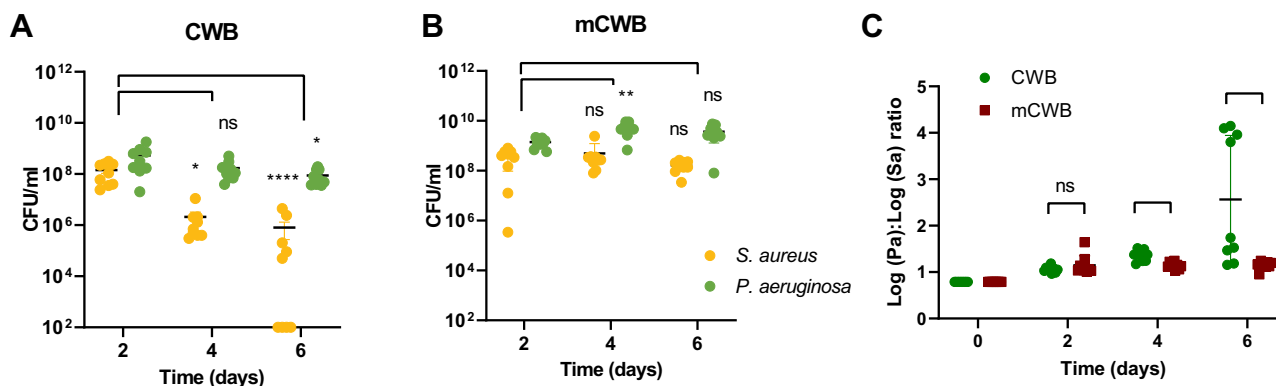


FIGURE 3 *Staphylococcus aureus* and *Pseudomonas aeruginosa* CFU data for untreated models over time in CWB and mCWB models. Panel A and B shows individual values, mean and standard deviation ($n = 9$) for both species. The data sets were tested for Gaussian distribution, but not all data sets were normally distributed. Therefore, Kruskal–Wallis tests were used with Dunn's multiple comparisons, including Dunn's correction to compare the CFUs at day 2 to the CFUs on day 4 and day 6. Limit of detection was 100 CFU/mL, hence if zero colonies were observed, this was plotted as 99 CFU/mL. Panel C shows the ratios between the two species in each model, which were calculated as $\log_{10}(\text{cfu})/\log_{10}(\text{cfu})$. Pairwise differences between the ratios at the different time points were tested using a two-tailed Mann–Whitney U test for non-parametric data.

After 2 days, microscopy was performed to visualise the distribution of the two bacteria species in the mature models and to investigate the formation of microcolonies. pH and oxygen measurements were obtained, to investigate how the mature biofilms had affected the microenvironment within the model. Finally, some models were harvested to establish a CFU count. The remaining models received one of six different treatments: Hydrogel A, Hydrogel B, Hydrogel C, CHX, placebo or untreated.

After 4 days, microscopy was performed on the untreated models to investigate whether the distribution of the two species had changed, as well as to visualise the overall distribution of live and dead bacteria. pH and oxygen measurements were obtained again, to investigate the effect of the treatments. Models of each treatment were harvested and enumerated for CFU counts. Some models were then re-treated. The remnants of the initial treatment were carefully removed without disrupting the model before new treatment was added.

After 6 days, the last models were evaluated using microscopy, pH and oxygen measurements, and CFU enumerations as described for day 4.

Every 24 h, the WSM in the wells of the 12-well-plate was exchanged with fresh media.

2.8 | Data analysis and statistics

For CFU enumerations and pH and oxygen measurements, three biological replicates (models made on different days, with different ON culture) containing three technical replicates (models made on the same day, with the same ON culture) were analysed, resulting in a total of nine samples ($n = 9$) of each.

All statistical analyses were performed using GraphPad Prism version 9. To denote statistical significance, the following symbols were applied: ns = not significant ($p > 0.05$), * $p < 0.05$, ** $p < 0.01$ and *** $p < 0.001$.

The lower limit of detection was 100 CFU/mL, so if no colonies were observed, this was consequently plotted as '99' for all statistical tests.

For comparing CFU numbers in untreated models over time, the data was initially tested for Gaussian distribution. Since the test did not confirm a normal distribution in all data sets, a Kruskal–Wallis test was performed together with Dunn's multiple comparisons including Dunn's correction. Mean pH values in each model over time were tested similarly.

To test the statistical significance of the various treatment effects a two-tailed Mann–Whitney U test for non-parametric data was used. The placebo hydrogel treatment was compared to the three hydrogels (hydrogel A, B and C) whilst the untreated models were compared to the CHX treated models. The tests were performed on raw data for CFU/mL. Pairwise comparison of oxygen flux rates and *P. aeruginosa*:*S. aureus* ratios were tested the same way.

Net consumption of O_2 in the models was estimated from gas fluxes of the measured steady state O_2 profiles, using a modified version of Fick's first law of diffusion,¹⁷

$$J = 0.5 \left(-D \frac{C_a - C_b}{X_a - X_b} \right) + 0.5 \left(-D \frac{C_b - C_c}{X_b - X_c} \right)$$

where J is the flux of O_2 ($\text{nmol } O_2 \text{ cm}^{-2} \text{ min}^{-1}$) through points a, b, c ; D is the diffusion coefficient of O_2 ($2.94 \times 10^{-5} \text{ cm}^2 \text{ s}^{-1}$; 33°C; 9 psu); C is the concentration of O_2 (μM), and X is the depth relative to the surface of the models (μm).

3 | RESULTS

3.1 | Growth of microbes in the models

In the original CWB model, *P. aeruginosa* numbers remained almost constant with a $< 1 \log_{10}$ reduction in CFU/mL from 2 days to 6 days

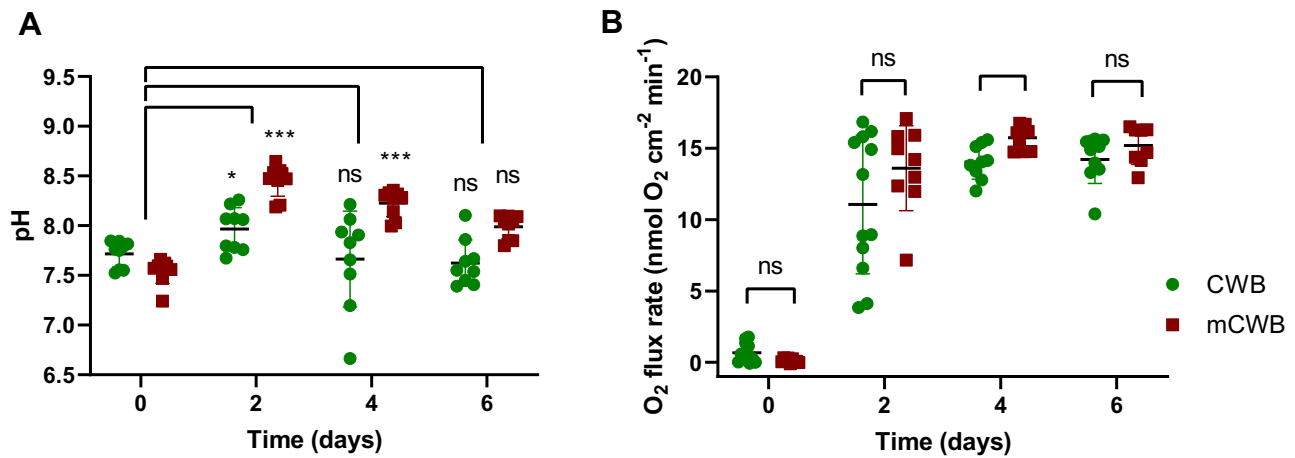


FIGURE 4 pH levels and oxygen flux rates in untreated models over time. Individual values, mean values and standard deviations are shown across all pH depth profiles ($n = 9$) in panel A. Individual values, mean values and standard deviations are shown for oxygen flux rates ($n = 9$) in panel B. Changes in pH were tested with a Kruskal–Wallis test with Dunn's multiple comparisons, including Dunn's correction to see significant changes in pH over time for each model. The data for day 0 was compared to data for day 2, 4 and 6. For O₂ flux, pairwise comparisons were performed to determine any significant differences between the two models, using a two-tailed Mann–Whitney U test for non-parametric data.

(Figure 3A). *S. aureus* decreased significantly from day 2 to day 4 with a $\sim 2 \log_{10}$ reduction in CFU/mL and then decreased further at day 6. In the mCWB model, *S. aureus* numbers remained constant for the duration of the experiments (Figure 3B). *P. aeruginosa* numbers increased significantly by $0.6 \log_{10}$ CFU/mL from day 2 to day 4, but then decreased again by day 6, resulting in no significant difference between the numbers at day 2 and day 6. In general, the CFUs in the mCWB were slightly higher than those observed for the original CWB.

The ratios between *P. aeruginosa* and *S. aureus* in the CWB model increased successively over the 6 days, resulting in a large *P. aeruginosa*:*S. aureus* ratio by day 6 (Figure 3C). In some untreated CWB models, *S. aureus* was completely outcompeted by *P. aeruginosa* at day 6. The ratios between *P. aeruginosa* and *S. aureus* in the mCWB also increased over the 6 days, but not to the same extent. By day 6, there were on average just over 20 *P. aeruginosa* per *S. aureus* in the mCWB model. The *P. aeruginosa*:*S. aureus* ratios in the two models differed significantly at day 4 and day 6, despite a large variation observed in the data for the CWB on day 6.

3.2 | pH and oxygen conditions in the untreated models

pH depth profiles were found to exhibit little or no depth gradients and averages across whole profiles were therefore calculated (Figure 4A). The pH in the original CWB had a baseline level of 7.7, which increased significantly after 2 days to 8.0 where after it decreased to 7.7 and remained stable at 7.7 until day 6 (Figure 4A). The baseline pH of the mCWB was 7.5, which increased significantly to 8.4 after 2 days. After 4 days, it had decreased to 8.2, still being significantly higher than the baseline pH. On day 6, the pH had further decreased to 8.0.

Oxygen flux rates at day 0 were close to zero as also visualised by the fully oxyc conditions inside the models (Figure 4B). At day 2, the flux increased to 11.1 ± 4.9 and 13.6 ± 3.0 for the CWB and mCWB, respectively and reached asymptotic flux rates at day 4 and 6. At days 2, 4, and 6, the oxygen flux rates were slightly higher in the mCWB, but only significantly so at day 4.

3.3 | Treatment effects on CFU in CWB and mCWB

In the CWB, hydrogel A indicated complete eradication after 2 days of treatment (Table 2). Hydrogel B eradicated all *S. aureus* after 2 days while $3.27 \log_{10}$ CFU/mL *P. aeruginosa* remained. After 2×2 days of treatment, all bacteria were eradicated. Hydrogel C caused a significant reduction of both species, with no colonies of *S. aureus* observed after the first 2 days of treatment. The number of CFUs did however increase again after 2×2 days of treatment with hydrogel C for *S. aureus*. CHX significantly reduced the number of *S. aureus*, compared to the untreated models after 2 days, but apparently increased the number of *P. aeruginosa*. After 2×2 days of treatment, there was no significant difference between CHX treated samples of either species compared to the untreated models, although *P. aeruginosa* still had slightly increased CFU numbers after CHX treatment.

In the mCWB, all of the hydrogels caused a significant reduction of CFUs for both species after 2 days of treatment as well as 2×2 days of treatment. However, none of them caused a complete eradication (Table 3). CHX had no significant effect on *S. aureus* after the first 2 days of treatment nor after 2×2 days of treatment. CHX did, however, cause a significant $1.4 \log_{10}$ reduction of *P. aeruginosa* compared to the untreated models. This effect was further increased to a $1.9 \log_{10}$ reduction after 2×2 days of treatment.

	Treatment effects			
	CWB: log ₁₀ CFU/mL			
	After 2 days of treatment		After 2 × 2 days of treatment	
	<i>S. aureus</i>	<i>P. aeruginosa</i>	<i>S. aureus</i>	<i>P. aeruginosa</i>
Untreated	6.00 ± 0.50	8.10 ± 0.34	4.00 ± 1.99	7.86 ± 0.29
Placebo	5.72 ± 0.55	7.73 ± 0.17	4.93 ± 2.45	7.18 ± 0.38
CHX 2%	3.01 ± 1.23 (***)	8.58 ± 0.09 (**)	3.52 ± 1.77 (ns)	8.10 ± 0.36 (ns)
Hydrogel A	<2 (***)	<2 (***)	<2 (**)	<2 (***)
Hydrogel B	<2 (***)	3.27 ± 1.28 (***)	<2 (**)	<2 (***)
Hydrogel C	<2 (***)	5.36 ± 0.73 (***)	2.16 ± 0.49 (**)	3.71 ± 1.86 (***)

Note: Data represented as mean of log₁₀ values ± SD (n = 9). The treatment effects were tested using two-tailed Mann–Whitney U test for non-parametric data. The placebo treatment was compared to all hydrogels (A, B and C) while the untreated models were compared to the CHX treated models. The following symbols were used to denote statistical significance: ns = not significant (p > 0.05), *p < 0.05, **p < 0.01, and ***p < 0.001. Tests were performed on raw, non-transformed data of CFU/mL. Lower limit of detection was 100 CFU/mL. If zero colonies were observed, this was plotted as 99 CFU/mL.

	Treatment effects			
	mCWB: log ₁₀ CFU/mL			
	After 2 days of treatment		After 2 × 2 days of treatment	
	<i>S. aureus</i>	<i>P. aeruginosa</i>	<i>S. aureus</i>	<i>P. aeruginosa</i>
Untreated	8.46 ± 0.42	9.62 ± 0.34	8.16 ± 0.27	9.38 ± 0.59
Placebo	9.26 ± 0.07	9.59 ± 0.11	9.28 ± 0.13	9.47 ± 0.19
CHX 2%	7.82 ± 1.16 (ns)	8.19 ± 0.81 (***)	8.15 ± 0.51 (ns)	7.53 ± 0.31 (***)
Hydrogel A	4.09 ± 1.66 (***)	4.08 ± 1.04 (***)	2.70 ± 0.92 (***)	4.10 ± 1.47 (***)
Hydrogel B	3.33 ± 1.14 (***)	5.74 ± 1.08 (***)	3.84 ± 1.82 (***)	4.84 ± 1.95 (***)
Hydrogel C	3.79 ± 1.75 (***)	6.76 ± 0.80 (***)	3.93 ± 1.74 (***)	5.56 ± 1.13 (***)

Note: Data represented as mean of log₁₀ values ± SD (n = 9). The treatment effects were tested using two-tailed Mann–Whitney U test for non-parametric data. The placebo treatment was compared to all hydrogels (A, B and C) while the untreated models were compared to the CHX treated models. The following symbols were used to denote statistical significance: ns = not significant (p > 0.05), *p < 0.05, **p < 0.01, and ***p < 0.001. Tests were performed on raw, non-transformed data of CFU/mL. Lower limit of detection was 100 CFU/mL. If zero colonies were observed, this was plotted as 99 CFU/mL.

3.4 | pH and oxygen gradients in treated and untreated CWB

The pH of the freshly inoculated CWB was stable at 7.8 and displayed only a small depth gradient (Figure 5). Oxygen concentration decreased slightly with increasing depth from a near air-saturated concentration (200 μM) at the air-model interface decreasing to 150 μM 1.5 mm inside the model. After 2 days, the bacterial effect on oxygen concentration was clear as a steep gradient had formed reaching anoxic conditions ~1 mm below the surface. pH remained stable at ~8 with no depth gradients.

The initial pH of the placebo hydrogel and CHX treatment was 6.5 and 5.9, respectively (Table 1). However, pH remained stable in the models with placebo treatment at 7.9 after 2 days of treatment and at 7.3 after another round of treatment (Figure 5). The pH for the

TABLE 2 Effect of various treatments on *Staphylococcus aureus* and *Pseudomonas aeruginosa* in the CWB after 2 days and 2 × 2 days of treatment as seen on day 4 and day 6.

TABLE 3 Effect of various treatments on *Staphylococcus aureus* and *Pseudomonas aeruginosa* in the mCWB after 2 days and 2 × 2 days of treatment as seen on day 4 and day 6.

CHX treated models was very similar with a pH of 7.5 after one round of treatment and 7.3 after the second round of treatment. The three hydrogel treatments resulted in acidic conditions in the entire model. The pH after the first treatment was 4.3, 3.8 and 4.0 for hydrogel A, B and C, respectively. Following another treatment, the pH decreased further, particularly for hydrogel B and C. On day 6, the pH was 3.9, 3.1 and 3.2 for hydrogel A, B and C respectively.

The oxygen concentrations within the wound models correlated with the killing efficacy of the applied treatments where low killing efficacy led to steeper oxygen gradients. The oxygen profiles for hydrogels A, B and C were similar to the baseline profile observed at day 0, suggesting low levels of O₂ consumption (Figure 5). The oxygen profile for CHX and the placebo hydrogel on day 4 and day 6 was similar to the oxygen gradient for the untreated models, but with a less steep concentration gradient. On day 6, oxygen penetrated deep into

CWB

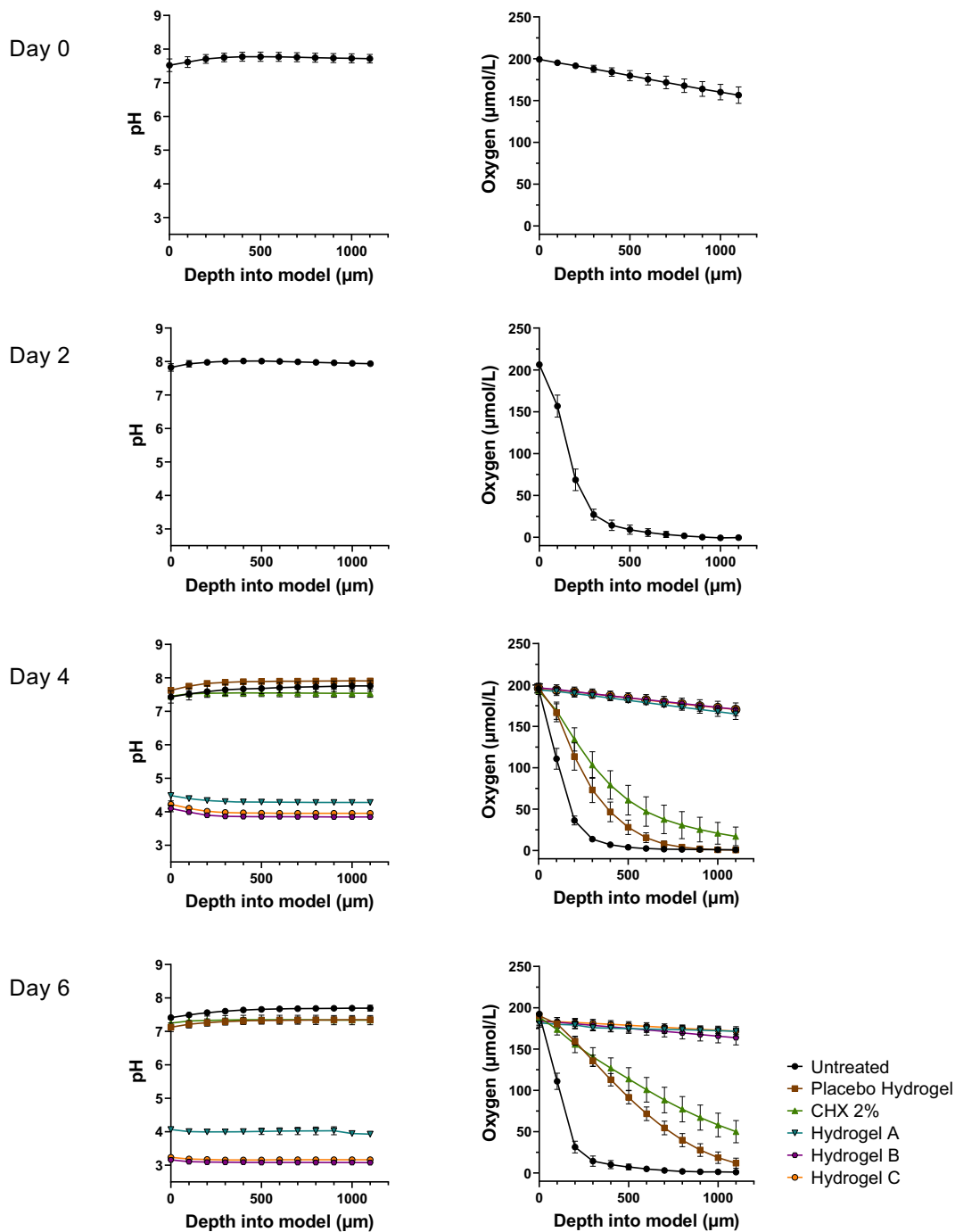


FIGURE 5 The pH and oxygen gradients in the CWB models over time. Mean values and standard deviations are shown ($n = 9$ for each condition and every time point). On day 0, the newly cast untreated models were measured as a baseline. On day 2, the bacterial effect on pH and oxygen of the untreated models was observed. On day 4 and day 6, the treatment effects on the pH and oxygen gradients were obtained as well as the gradients of untreated models. (To see these graphs with individual data points see Supporting Information.)

the models treated with CHX and placebo, causing a less steep gradient, despite the number of CFUs being similar to or larger than the number of CFUs in the untreated models. Anoxic conditions in the untreated models were reached at 0.6 mm depth on day 4 and at 0.8 mm depth on day 6.

3.5 | pH and oxygen gradients in treated and untreated mCWB

Similar trends were observed in the mCWB as in the original model. pH in the untreated models increased from 7.6 on day 0 to

mCWB

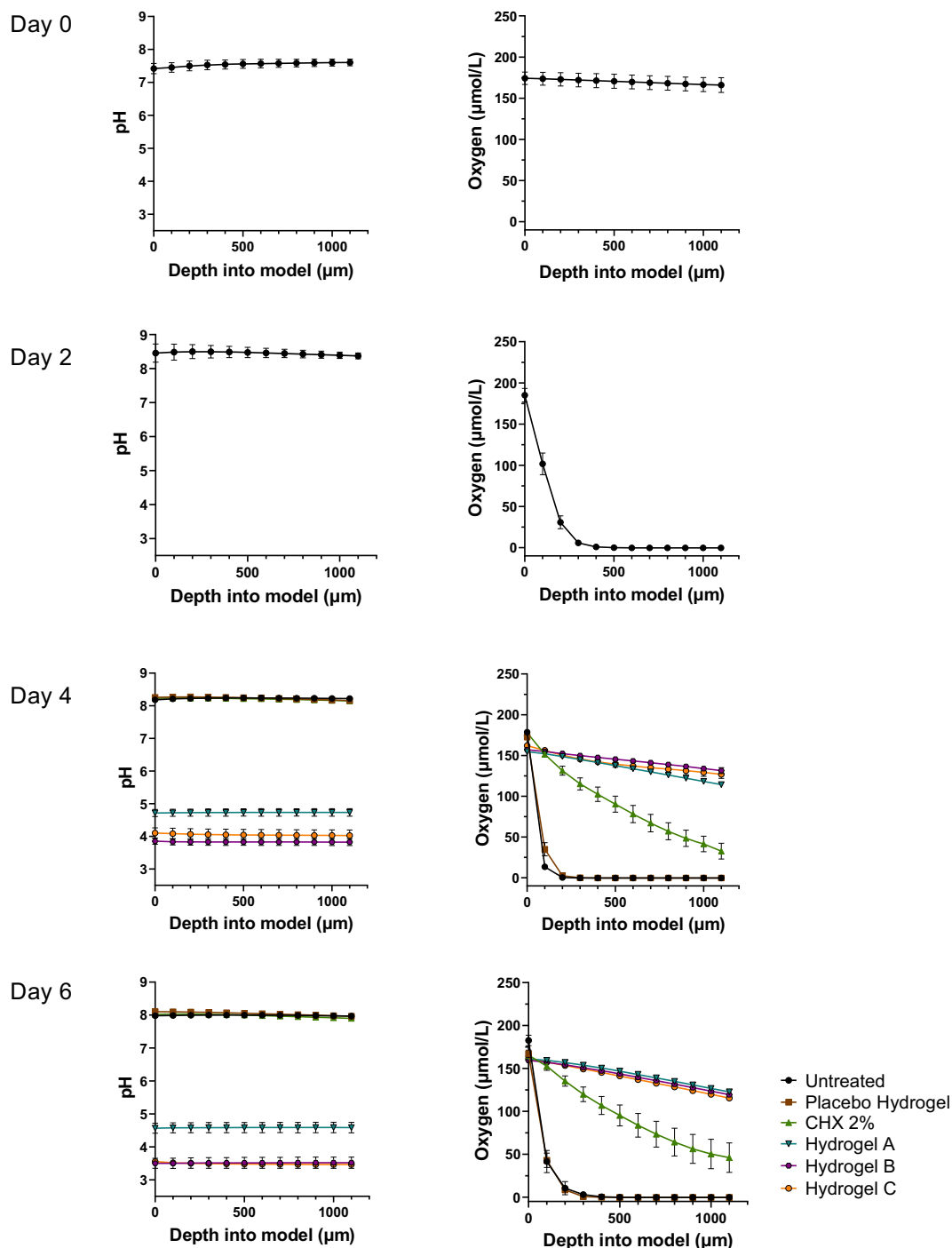


FIGURE 6 The pH and oxygen gradients in the mCWB models over time. Mean values and standard deviations are shown ($n = 9$ for each condition and every time point). On day 0, the newly cast untreated models were measured as a baseline. On day 2, the bacterial effect on pH and oxygen of the untreated models was observed. On day 4 and day 6, the treatment effects on the pH and oxygen gradients were obtained as well as the gradients of untreated models. (To see these graphs with individual data points see Supporting Information.)

8.4 on day 2 with no depth gradients (Figure 6). On day 0, the model did not display any O_2 gradients but following 2 days of incubation, bacterial respiration resulted in anoxic conditions at a depth of 0.4 mm.

The placebo and CHX treatments had no effect on the pH, and both treatments displayed similar levels as the untreated models, with a pH of 8.2 on day 4 and 8.0 on day 6. The three hydrogels decreased the pH to 4.7, 3.8 and 4.0 for hydrogels A, B and C, respectively on day 4. On day

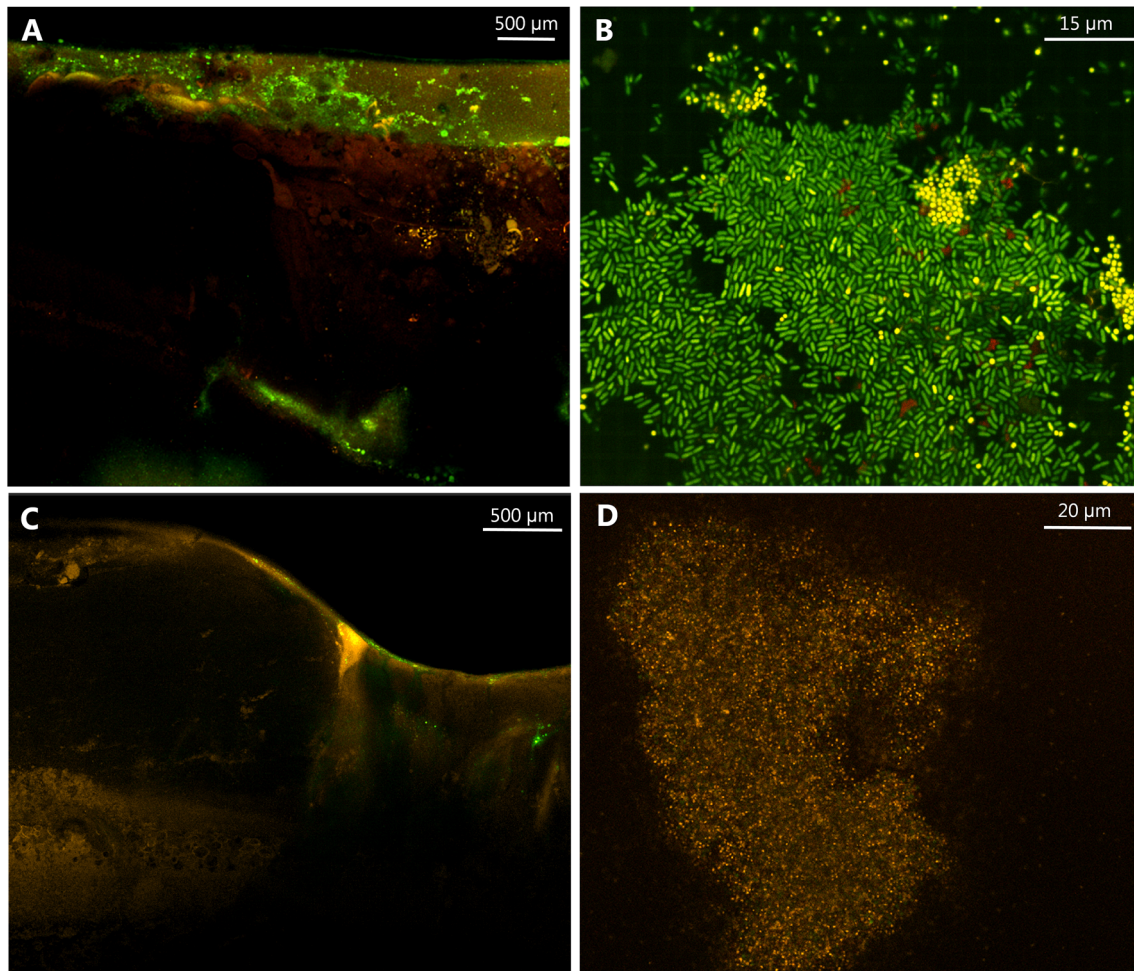


FIGURE 7 Overview of the CWB on day 2 (A) and day 4 (C). Colonies of both *Staphylococcus aureus* and *Pseudomonas aeruginosa* were observed at day 2 (B). Aggregates of dead *S. aureus* could be observed on day 4 (D). Live bacteria = green, dead bacteria = orange.

6, the pH level for models treated with hydrogel A had decreased slightly to 4.6. Hydrogel B and C both caused a pH level of 3.5 on day 6, which was not quite as low as observed in the original CWB.

The oxygen gradients on day 4 and 6 for the placebo treatment were identical to those of the untreated models, reflecting the very similar numbers of CFUs between the two (Figure 6). Anoxic conditions in the untreated models were reached at 0.2 mm depth on day 4 and at 0.4 mm depth on day 6. The CHX treatment reduced the number of viable bacteria slightly and resultantly a less steep oxygen gradient was observed on both day 4 and day 6. For all three hydrogels, the oxygen concentration gradients on day 4 and 6 were very similar to the baseline treatment, corresponding to a significant reduction in CFUs observed for all three treatments.

3.6 | Formation of microcolonies in the models

After 2 days, microcolonies of the two species had formed in the CWB model (Figure 7B). Both *P. aeruginosa* and *S. aureus* were observed in the top and deeper into the model (Figure 7A). On day 4, live *S. aureus* were difficult to locate, only a few were observed in

the middle of the model. Instead, many aggregates of dead *S. aureus* could be observed (Figure 7D). Live *P. aeruginosa* were still found within the model, primarily at the top layers.

After 2 days the mCWB model contained microcolonies of both species together with larger aggregates (Figure 8B). *P. aeruginosa* was observed primarily in the top part of the model. *S. aureus* was observed in the top as well as in the middle of the model all the way down to the bottom edge (Figure 8A). After 4 days in the mCWB model, *P. aeruginosa* had grown to a dominant presence in the top of the model. *S. aureus* was present in large biofilm aggregates in the top, but also in the deeper layers, as well as in the bottom of the model in the middle (Figure 8C). On day 6 large biofilms of both species were still observed as well as smaller microcolonies (Figure 8E,F).

4 | DISCUSSION

4.1 | The creation of the mCWB

The main objective of this study was to create a scaffold displaying wound-like characteristics, on which topical wound treatments could

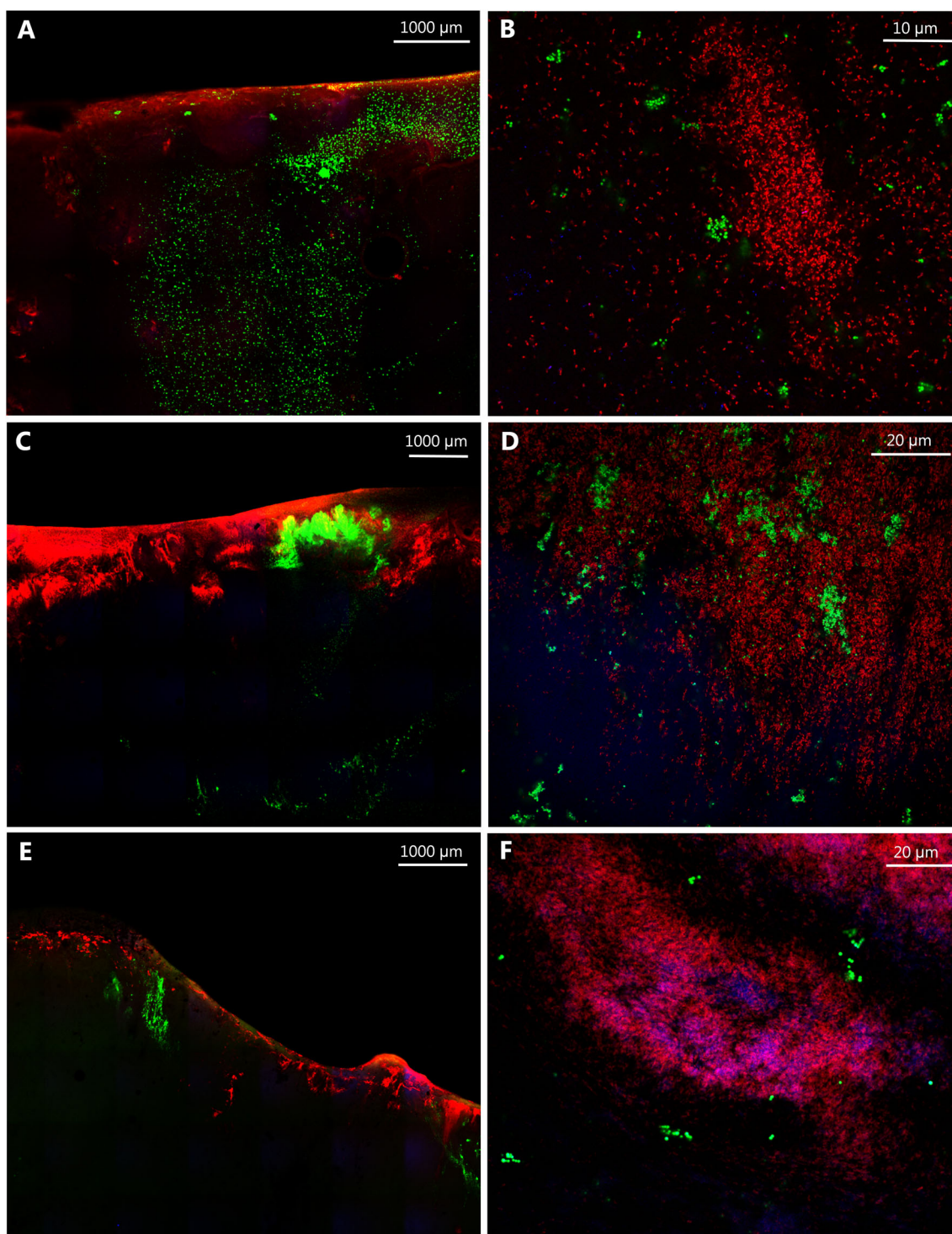


FIGURE 8 Overview of the mCWB on day 2 (A), day 4 (C) and day 6 (E). Microcolonies of both *Staphylococcus aureus* and *Pseudomonas aeruginosa* were observed on all days: on day 2 (B), day 4 (D) and day 6 (F). *S. aureus* = green, *P. aeruginosa* = red, dead bacteria = blue.

be tested. This was done in part by replacing agar with collagen as the support matrix of an existing in vitro model, as collagen has been used previously to grow wound-relevant biofilms¹⁸ and to mimic soft tissue infections.^{19–21} Although differences between agar and collagen have yet to be evaluated extensively, some fundamental differences between the two matrix materials do exist. Agar is a kelp-derived,

polar carbohydrate²² previously found to interfere with certain antibiotic compounds,²³ whereas collagen is a fibrous protein abundant in the skin of humans, and other mammals.²⁴ Collagen is relatively hydrophobic, generally non-polar, and has previously been observed to promote antimicrobial tolerance, as well as a change in the ratios of the extracellular polymeric substances (EPS) contents of bacterial

biofilms.^{25–27} We made a decision to only include type 1 collagen in our model, as it is the most abundant protein of the skin, well knowing that human skin contains several different types of collagen, as well as other proteins such as fibrin and elastin.²⁸ We speculate that the inclusion of collagen in our modified model could have had an effect on the EPS produced by the two microorganisms and that this change in EPS could affect the tolerance of the microbes. Although agar has been considered the gold standard of matrix materials due to its ease of use and low cost, alternatives such as poloxamer hydrogels²⁹ and cellulose³⁰ have previously been applied to mimic *in vivo*-like wound conditions. Various types of semi-solid models have been employed for growing non-surface attached bacteria distributed in distinct biofilm aggregates.³¹ In addition to a support matrix, the inclusion of a wound-like medium is also important as the components of such media can affect biofilm formation as well as tolerance toward antimicrobials.^{18,32,33} For example, Pitten et al.³⁴ found that the presence of albumin and defibrinated sheep blood reduced the efficiency of a range of antiseptics against common pathogens. Finally, physiological levels of amylase of 140 U/L, were added to the modified model.³⁵ This was done to dissolve the biodegradable starch microspheres that completely degrade in α -amylase. Amylase is an enzyme that catalyses the hydrolysis of starch into sugars and has either salivary or pancreatic origin, and raised levels of amylase have previously been correlated with complications in wound healing.³⁶

Antimicrobial tests are often conducted for 24 h, although the effect of a single treatment over several days or continuous treatment over longer periods can be of relevance, particularly in terms of resistance development. In these cases, an *in vitro* model able to sustain prolonged growth of bacteria is required, which may be accomplished by a continuous exchange of media over several days.^{21,37} Moreover, while bacterial species in chronic wounds have been found to fluctuate in abundance over time, several studies agree that chronic wounds are polymicrobial.^{38–41} Steady-state communities of bacteria *in vitro* are often grown in liquid incubators and are therefore not suitable for testing topical treatments. Furthermore, shear flow is often present in liquid incubators, which causes a distinctively different biofilm.⁴² Continuously adding nutrients, without introducing shear flow is not a simple task but has been proposed previously, for example, by facilitating nutrient and waste exchange using perforated tubing.⁴³ Alternatively, incubators have been designed where media enters the system by basal perfusion.⁴⁴ For the present study, it was decided to use transwell inserts, an idea inspired by Price et al.²⁰ This presented a simple solution for sequential media exchange, which allowed us to test treatment effects over longer periods. However, in some cases contamination in the 0.4 μm filter separated media-reservoir beneath the models was observed. When subjected to treatment, it has been observed that both *P. aeruginosa* and *S. aureus* can reduce in size and this could have caused them to escape through the filter.⁴⁵ We warrant that this may have provided a reservoir of viable bacteria in the nutrient chamber of the modified models, which potentially could have migrated back into the model when conditions were more favourable.

The formation of gradients in nutrients, oxygen and pH is in part created by bacteria but can in turn also lead to a heterogenic distribution of bacterial aggregates as well as spatial variations in bacterial activities and growth.^{46–48} Especially differences in growth rates have previously been shown to play a role in antimicrobial tolerance⁴⁹ where certain antibiotics target metabolic active processes, rendering non- or slow-growing bacteria unsusceptible.^{50,51} In the mCWB model, it was demonstrated that an alkaline pH of >8.0 was maintained over 6 days of incubation simulating a non-healing environment. Furthermore, steep gradients of O₂ concentration quickly established leading to a shallow top zone continuously exposed to O₂ from the atmosphere while the major part of the model was anoxic, mimicking *in vivo* conditions. Oxygen was only measured in the middle part of the model which represented the wound bed. A small pilot study (data not shown) was performed which measured oxygen at both the void of the model and the edge of the void of untreated models. No difference was observed, hence we decided not to perform both measurements throughout further experiments. Yet, in the future, measuring oxygen concentrations at both the middle and the edge of the model might be warranted, as oxygen measurements at the edge of the wound might provide further information regarding the various treatment effects.

4.2 | The original CWB versus the mCWB model

From the analyses made in the present study it can be argued that the mCWB model has the advantages that (i) a stable ratio of the two bacterial species *P. aeruginosa* and *S. aureus* can be retained, (ii) exchange of media is facilitated without shear flow, and (iii) an alkaline pH can be maintained for a longer period of time.

The mCWB model retained a stable ratio of the two species over time, compared to the original CWB model, and we initially suspected that the continuous addition of nutrients played a role. However, this was disproved in supplementary experiments (see further below). The incorporation of collagen instead of agar may also have affected the growth of both species. A few studies comparing growth of human cell lines in collagen versus agar have found improved growth in collagen.^{52,53} Additionally, *S. aureus* can grow in a broader pH range than *P. aeruginosa* (*S. aureus* range: 4.0–10.0, *P. aeruginosa* range: 4.5–9.5^{54,55}), why the slightly more alkaline pH observed in the untreated mCWB models could indicate a growth advantage for *S. aureus*. However, this remains speculative. Finally, the microscope images suggested that *S. aureus* was found in areas free from *P. aeruginosa*. Surprisingly, *S. aureus* was present in deeper layers in the mCWB, although it was described to reside in the top layers in the original CWB, as previously observed in chronic wounds.⁵⁶ We hypothesize that, since *P. aeruginosa* invaded the top layers of the model, perhaps seeking the benefit of high oxygen levels, *S. aureus* proliferated instead in the bottom of the model, maybe to avoid competition and instead benefitted from being close to the nutrient source. It should be noted that neither of the *in vitro* models contains a reactive

immune response, which would arrive from within the wound and inevitably also affect the distribution of the two species.

As previously described, chronic non-healing wounds are found to be alkaline, and the mCWB maintained a more alkaline pH for a longer period of time compared to the original CWB model. This was somewhat surprising, since the mCWB contained phosphate buffer instead of physiological saline. One explanation for the higher pH could be due to the higher number of bacteria in the model, as both *S. aureus* and *P. aeruginosa* are known to increase the pH in tissue.⁵⁷ Another reason could be the continuous addition of nutrients to the mCWB, presenting the residing bacteria with more substrate which could potentially be converted into ammonia or other alkaline compounds increasing the pH.⁵⁸ The addition of collagen instead of agar could also affect the pH, as collagen is stepwise reduced to amino acids increasing the pH²⁸ and both *S. aureus* and *P. aeruginosa* have been found to produce collagenolytic enzymes.²⁴

Even though oxygen displays similar effective diffusion coefficients in collagen and agar,^{59,60} slightly higher oxygen fluxes were observed in the untreated mCWB models. In addition, the oxygen penetration depth was lower in the untreated mCWB compared to the original CWB model. This was probably due to the slightly higher number of bacteria as well as the deeper distribution of bacteria in the mCWB model.

4.3 | The effect of adding nutrients

Although several modifications were made to the original model, it was questioned if the effect of adding nutrients could account for most or all of the observed differences between the CWB and the mCWB. Therefore, supplementary experiments were performed in which continuous nutrients were added to the original CWB but removed from the mCWB (see Supporting Information).

The mCWB displayed the same stability between species in untreated models regardless of if nutrients were added or not (Figure S1). The ratio between the two species in the original CWB model was even more skewed when nutrients were added continuously. This disproved our hypothesis that the addition of nutrients to the mCWB was the main cause of the obtained species stability. However, continuously adding nutrients to the original CWB did increase the survival of both species for all hydrogel treatments (Figure S2). For the mCWB, removal of continuous nutrients caused a more pronounced killing effect of the hydrogel treatments. We speculate that the effects observed for both models were due to the altered pH reductions observed (Figure S3): Continuously adding nutrients to the CWB caused a less pronounced pH reduction by the hydrogel treatments, while removing continuous nutrients from the mCWB caused a more pronounced pH reduction for the three hydrogels. Hence, while the addition of nutrients to the models seemed to have an effect on the survival against treatments due to pH alternations, it was not the main modification that played a role in terms of species stability in the two models.

4.4 | Potential of new wound care products

We speculate that the differences between the two models listed here, resulted in a less pronounced effect of the hydrogels in the mCWB model than in the original CWB model. The phosphate-buffered system of the mCWB could potentially alleviate the decrease in pH created by the hydrogels as was seen in the original CWB model possibly impacting the killing efficiency. Additionally, the media in the mCWB model was continuously exchanged possibly diluting the effect of the hydrogels. However, in both wound models the hydrogels decreased the pH after 2 days of treatment and restored the oxygen levels back to baseline, despite the differences in bacterial eradication between the two models. The acidification of the wound milieu is a highly desired quality of the products, as natural healing processes within wounds are associated with low pH and an alkaline pH has been shown to be correlated with impaired healing.⁵⁸ Restoring oxygenation by preventing bacterial respiration within the wound is also a favourable quality of the products, as oxygen is a necessity for successful wound healing.⁶¹ The oxygen level within a wound is associated with several facets of healing as it impacts (i) the growth of the resident bacteria, (ii) the efficacy of antimicrobials, (iii) cellular functions, reparative processes and the immune system where polymorphonuclear neutrophils in particular require oxygen for their respiratory bursts.^{62,63}

CHX was included as a positive control, as it is a commonly used antiseptic previously found to be active against both *S. aureus* and *P. aeruginosa*.¹⁴ Yet, in this study, CHX had a limited effect on bacterial numbers. Surprisingly, oxygen profiles reflecting lower respiration were observed for CHX treated models despite no or little reduction in the number of CFUs. CHX has previously been found to act bacteriostatic in low concentrations,⁶⁴ so we speculate that only low concentrations of CHX have reached the microbes in the models, possibly decreasing bacterial respiration, but leading to no CFU reduction.

5 | CONCLUSION AND PERSPECTIVES

Here, we presented a modified version of an existing in vitro model that fulfilled eight proposed criteria of an 'ideal' in vitro infected chronic wound model. It contained WSM, it was based on a collagen matrix providing a semi-solid environment, nutrients were continuously added without creating shear flow within the model, it expressed several types of 3D gradients, and it contained no non-mammalian components or solid surfaces on which the biofilm could grow.

The established model maintained a stable ratio of *S. aureus* and *P. aeruginosa* over 6 days. Moreover, it expressed alkaline conditions with a pH level ≥ 8.0 and steep oxygen gradients resulting in an anoxic microenvironment, which is similar to the conditions observed in chronic wounds. Hence, it provided a scaffold onto which topical wound treatments could be tested under in vivo-like conditions.

The three topical hydrogels tested here all displayed a significant reduction in the numbers of CFUs. Moreover, they decreased the pH

resulting in acidic conditions and they decreased bacterial oxygen consumption, which are both qualities desired for a topical wound healing product. It is very common to only measure the effect of new antimicrobial treatments by evaluating the surviving pathogens. We advocate that changes in the microenvironment, such as oxygen levels or pH that may aid in healing processes should also be considered.

In vitro models will never correspond completely to the clinical situation. There will always be certain limitations, such as a lacking immune response or being able to see an organism as a whole. However, in vitro models are still a valuable tool in the early phases of evaluating new treatments and it is therefore important to continue improving upon the currently used in vitro models. The model presented here could potentially be improved by the addition of human skin cells or human immune cells. Moreover, a more complex WSM could be created, as has recently been done in other studies.⁶⁵ Further confirmation studies could be performed using RNA-sequencing to see the transcriptomic behaviour of the residing bacteria and compare this to RNA-sequencing data from bacteria obtained from clinical samples.

ACKNOWLEDGEMENTS

ICT is funded by Magle Chemoswed AB, through a non-restricted research grant. The study was supported by grants from the Novo Nordic Foundation through grants NNF19OC0056411 (TB) and NNF19OC0054390 (TB). The funding sources were not involved in the study design, in the collection, analysis and interpretation of data, in the writing of the report, or in the decision to submit the article for publication.

DATA AVAILABILITY STATEMENT

The data that support the findings of this study are available from the corresponding author upon reasonable request.

ORCID

Ida C. Thaarup  <https://orcid.org/0000-0001-9004-0978>

Mads Lichtenberg  <https://orcid.org/0000-0002-0675-4554>

Trine R. Thomsen  <https://orcid.org/0000-0002-7393-9372>

REFERENCES

- Shi D, Mi G, Wang M, Webster TJ. In vitro and ex vivo systems at the forefront of infection modeling and drug discovery. *Biomaterials*. 2019;198:228-249. doi:10.1016/j.biomaterials.2018.10.030
- Cooper R, Bjarnsholt T, Alhede M. Biofilms in wounds: a review of present knowledge. *J Wound Care*. 2014;23:570-582. doi:10.12968/jowc.2014.23.11.570
- Frykberg RG, Banks J. Challenges in the treatment of chronic wounds. *Adv Wound Care*. 2015;4:560-582. doi:10.1089/wound.2015.0635
- Thaarup IC, Bjarnsholt T. Current in vitro biofilm-infected chronic wound models for developing new treatment possibilities. *Adv Wound Care*. 2021;10:91-102. doi:10.1089/wound.2020.1176
- Chen X, Lorenzen J, Xu Y, et al. A novel chronic wound biofilm model sustaining coexistence of *Pseudomonas aeruginosa* and *Staphylococcus aureus* suitable for testing of antibiofilm effect of antimicrobial solutions and wound dressings. *Wound Repair Regen*. 2021;29:820-829. doi:10.1111/wrr.12944
- Sun Y, Dowd SE, Smith E, Rhoads DD, Wolcott RD. In vitro multispecies Lubbock chronic wound biofilm model. *Wound Repair Regen*. 2008;16:805-813. doi:10.1111/j.1524-475X.2008.00434.x
- Gethin G. The significance of surface pH in chronic wounds palliative wound care view project management of patients with venous leg ulcers view project. *Wounds*. 2007;3:52-55. <https://www.researchgate.net/publication/265530186>
- James GA, Ge Zhao A, Usui M, et al. Microsensor and transcriptomic signatures of oxygen depletion in biofilms associated with chronic wounds. *Wound Repair Regen*. 2016;24:373-383. doi:10.1111/wrr.12401
- Bjarnsholt T, Alhede M, Alhede M, et al. The in vivo biofilm. *Trends Microbiol*. 2013;21:466-474. doi:10.1016/j.tim.2013.06.002
- Jensen P, Kolpen M, Kragh KN, Kühl M. Microenvironmental characteristics and physiology of biofilms in chronic infections of CF patients are strongly affected by the host immune response. *APMIS*. 2017;125:276-288. doi:10.1111/apm.12668
- Kirketerp-Møller K, Stewart PS, Bjarnsholt T. The zone model: a conceptual model for understanding the microenvironment of chronic wound infection. *Wound Repair Regen*. 2020;28:593-599. doi:10.1111/wrr.12841
- Kolpen M, Hansen CR, Bjarnsholt T, et al. Polymorphonuclear leukocytes consume oxygen in sputum from chronic *Pseudomonas aeruginosa* pneumonia in cystic fibrosis. *Thorax*. 2010;65:57-62. doi:10.1136/thx.2009.114512
- Dini V, Salvo P, Janowska A, Di Francesco F, Barbini A, Romanelli M. Correlation between wound temperature obtained with an infrared camera and clinical wound bed score in venous leg ulcers. *Wounds*. 2015;27:274-278. doi:10.1021/jp302401j
- Lipsky BA, Hoey C. Topical antimicrobial therapy for treating chronic wounds. *Clin Infect Dis*. 2009;49:1541-1549. doi:10.1086/644732
- Lipsky BA, Dryden M, Gottrup F, Nathwani D, Seaton RA, Stryja J. Antimicrobial stewardship in wound care: a position paper from the British society for antimicrobial chemotherapy and European wound management association. *J Antimicrob Chemother*. 2016;71:3026-3035. doi:10.1093/jac/dkw287
- Zamany A, Spångberg LSW. An effective method of inactivating chlorhexidine. *Endodontics*. 2002;93:617-620. doi:10.1067/moe.2002.122346
- De Beer D, Stoodley P. Microbial biofilms. *Prokaryotes Appl Bacteriol Biotechnol*. 2013;1:343-372. doi:10.1007/978-3-642-31331-8_32
- Werthén M, Henriksson L, Jensen PØ, Sternberg C, Givskov M, Bjarnsholt T. An in vitro model of bacterial infections in wounds and other soft tissues. *APMIS*. 2010;118:156-164. doi:10.1111/j.1600-0463.2009.02580.x
- Hakonen B, Lönnberg LK, Larkö E, Blom K. A novel qualitative and quantitative biofilm assay based on 3D soft tissue. *Int J Biomater*. 2014;2014:1-5. doi:10.1155/2014/768136
- Price BL, Lovering AM, Bowling FL, Dobson CB. Development of a novel collagen wound model to simulate the activity and distribution of antimicrobials in soft tissue during diabetic foot infection. *Antimicrob Agents Chemother*. 2016;60:6880-6889. doi:10.1128/aac.01064-16
- Slade EA, Thorn RMS, Young A, Reynolds DM. An in vitro collagen perfusion wound biofilm model: with applications for antimicrobial studies and microbial metabolomics. *BMC Microbiol*. 2019;19:1-13. doi:10.1186/s12866-019-1682-5
- Rhein-Knudsen N, Meyer AS. Chemistry, gelation, and enzymatic modification of seaweed food hydrocolloids. *Trends Food Sci Technol*. 2021;109:608-621. doi:10.1016/j.tifs.2021.01.052
- Hanus FJ, Sands JG, Benneti E. Antibiotic activity in the presence of agar. *Appl Microbiol*. 1967;15:31-34.

24. Harrington DJ. Bacterial collagenases and collagen-degrading enzymes and their potential role in human disease. *Infect Immun*. 1996;64:1885-1891.
25. Wallace DG, Rosenblatt J. Collagen gel systems for sustained delivery and tissue engineering. *Adv Drug Deliv Rev*. 2003;55:1631-1649. doi:10.1016/j.addr.2003.08.004
26. Ali IAA, Cheung BPK, Yau JYY, et al. The influence of substrate surface conditioning and biofilm age on the composition of *Enterococcus faecalis* biofilms. *Int Endod J*. 2020;53:53-61. doi:10.1111/iej.13202
27. Rahman MU, Fleming DF, Sinha I, Rumbaugh KP, Gordon VD, Christopher GF. Effect of collagen and EPS components on the viscoelasticity of *Pseudomonas aeruginosa* biofilms. *Soft Matter*. 2021;17:6225-6237. doi:10.1039/d1sm00463h
28. Duarte AS, Correia A, Esteves AC. Bacterial collagenases – a review. *Crit Rev Microbiol*. 2016;42:106-126. doi:10.3109/1040841X.2014.904270
29. Percival SL, Bowler PG, Dolman J. Antimicrobial activity of silver-containing dressings on wound microorganisms using an in vitro biofilm model. *Int Wound J*. 2007;4:186-191. doi:10.1111/j.1742-481X.2007.00296.x
30. Townsend EM, Sherry L, Rajendran R, et al. Development and characterisation of a novel three-dimensional inter-kingdom wound biofilm model. *Biofouling*. 2016;32:1259-1270. doi:10.1080/08927014.2016.1252337
31. Crone S, Garde C, Bjarnsholt T, Alhede M. A novel *in vitro* wound biofilm model used to evaluate low-frequency ultrasonic-assisted wound debridement. *J Wound Care*. 2015;24:64-72. doi:10.12968/jowc.2015.24.2.64
32. Kapalschinski N, Seipp HM, Onderdonk AB, et al. Albumin reduces the antibacterial activity of polyhexanide-biguanide-based antiseptics against *Staphylococcus aureus* and MRSA. *Burns*. 2013;39:1221-1225. doi:10.1016/j.burns.2013.03.003
33. She P, Chen L, Qi Y, et al. Effects of human serum and apo-transferrin on *Staphylococcus epidermidis* RP62A biofilm formation. *Microbiology*. 2016;5:957-966. doi:10.1002/mbo3.379
34. Pitten F-A, Werner H-P, Kramer A. A standardized test to assess the impact of different organic challenges on the antimicrobial activity of antiseptics. *J Hosp Infect*. 2003;55:108-115. doi:10.1016/S0195-6701(03)00260-3
35. Hasosah M, Masawa L, Jan A, Alsalem K. A case report of childhood recurrent autoimmune pancreatitis: a rare emerging entity. *J Clin Diagn Res*. 2016;10:SD01-SD02. doi:10.7860/JCDR/2016/18437.7917
36. Larsen LR, Schuller DE. Wound amylase levels as an early indicator of orocutaneous fistulae. *Laryngoscope*. 1984;94:1302-1306. doi:10.1288/00005537-198410000-00008
37. Kinniment SL, Wimpenny JWT, Adams D, Marsh PD. Development of a steady-state oral microbial biofilm community using the constant-depth film fermenter. *Microbiology*. 1996;142:631-638. doi:10.1099/13500872-142-3-631
38. Thomsen TR, Aasholm MS, Rudkj bing VB, et al. The bacteriology of chronic venous leg ulcer examined by culture-independent molecular methods. *Wound Repair Regen*. 2010;18:38-49. doi:10.1111/j.1524-475X.2009.00561.x
39. Tipton CD, Mathew ME, Wolcott RA, Wolcott RD, Kingston T, Phillips CD. Temporal dynamics of relative abundances and bacterial succession in chronic wound communities. *Wound Repair Regen*. 2017;25:673-679. doi:10.1111/wrr.12555
40. Johani K, Malone M, Jensen S, et al. Microscopy visualisation confirms multi-species biofilms are ubiquitous in diabetic foot ulcers. *Int Wound J*. 2017;14:1160-1169. doi:10.1111/iwj.12777
41. Kvich L, Burm lle M, Bjarnsholt T, Lichtenberg M. Do mixed-species biofilms dominate in chronic infections?—Need for in situ visualization of bacterial organization. *Front Cell Infect Microbiol*. 2020;10:396. doi:10.3389/fcimb.2020.00396
42. Roberts AEL, Kragh KN, Bjarnsholt T, Diggle SP. The limitations of in vitro experimentation in understanding biofilms and chronic infection. *J Mol Biol*. 2015;427:3646-3661. doi:10.1016/j.jmb.2015.09.002
43. Phan J, Ranjbar S, Kagawa M, Gargus M, Hochbaum AI, Whiteson KL. Thriving under stress: *Pseudomonas aeruginosa* outcompetes the background polymicrobial community under treatment conditions in a novel chronic wound model. *Front Cell Infect Microbiol*. 2020;10:1-13. doi:10.3389/fcimb.2020.569685
44. Oates A, Lindsay S, Mistry H, Ortega F, McBain AJ. Modelling anti-sepsis using defined populations of facultative and anaerobic wound pathogens grown in a basally perfused biofilm model. *Biofouling*. 2018;34:507-518. doi:10.1080/08927014.2018.1466115
45. Gaveau A, Coetsier C, Roques C, Bacchin P, Dague E, Causserand C. Bacteria transfer by deformation through microfiltration membrane. *J Membr Sci*. 2017;523:446-455. doi:10.1016/j.memsci.2016.10.023
46. Stewart PS, Franklin MJ. Physiological heterogeneity in biofilms. *Nat Rev Microbiol*. 2008;6:199-210. doi:10.1038/nrmicro1838
47. S nderholm M, Bjarnsholt T, Alhede M, et al. The consequences of being in an infectious biofilm: microenvironmental conditions governing antibiotic tolerance. *Int J Mol Sci*. 2017;18:2688. doi:10.3390/ijms18122688
48. Lichtenberg M, Jakobsen TH, K hl M, Kolpen M, Jensen P , Bjarnsholt T. The structure-function relationship of *Pseudomonas aeruginosa* in infections and its influence on the microenvironment. *FEMS Microbiol Rev*. 2022;46:1-13. doi:10.1093/femsre/fuac018
49. Xu KD, Stewart PS, Xia F, Huang CT, McFeters GA. Spatial physiological heterogeneity in *Pseudomonas aeruginosa* biofilm is determined by oxygen availability. *Appl Environ Microbiol*. 1998;64:4035-4039.
50. Walters MC III, Roe F, Bugnicourt A, et al. Contributions of antibiotic penetration, oxygen limitation, and low metabolic activity to tolerance of *Pseudomonas aeruginosa* biofilms to ciprofloxacin and tobramycin. *Antimicrob Agents Chemother*. 2003;47:1. doi:10.1128/AAC.47.1.317-323.2003
51. Borriello G, Werner E, Roe F, Kim AM, Ehrlich GD, Stewart PS. Oxygen limitation contributes to antibiotic tolerance of *Pseudomonas aeruginosa* in biofilms. *Antimicrob Agents Chemother*. 2004;48:2659-2664. doi:10.1128/AAC.48.7.2659-2664.2004
52. Dobo I, Allegraud A, Navenot JM, Boasson M, Bidet JM, Praloran V. Collagen matrix: an attractive alternative to agar and methylcellulose for the culture of hematopoietic progenitors in autologous transplantation products. *J Hematother Stem Cell Res*. 1995;4:281-287. doi:10.1089/scd.1.1995.4.281
53. Miao Z, Lu Z, Wu H, et al. Collagen, agarose, alginate, and Matrigel hydrogels as cell substrates for culture of chondrocytes in vitro: a comparative study. *J Cell Biochem*. 2018;119:7924-7933. doi:10.1002/jcb.26411
54. Stewart C. *Staphylococcus aureus* and staphylococcal enterotoxins. In: Ad H, ed. *Foodborne Microorg. Public Heal. Significance*. 6th ed. Australian Institute of Food Science and Technology; 2003:2003.
55. Klein S, Lorenzo C, Hoffmann S, et al. Adaptation of *Pseudomonas aeruginosa* to various conditions includes tRNA-dependent formation of alanyl-phosphatidylglycerol. *Mol Microbiol*. 2009;71:551-565. doi:10.1111/j.1365-2958.2008.06562.x
56. Fazli M, Bjarnsholt T, Kirketerp-M ller K, et al. Nonrandom distribution of *Pseudomonas aeruginosa* and *Staphylococcus aureus* in chronic wounds. *J Clin Microbiol*. 2009;47:4084-4089. doi:10.1128/JCM.01395-09
57. Bullock AJ, Garcia M, Shepherd J, Rehman I, Sheila M. Bacteria induced pH changes in tissue-engineered human skin detected non-invasively using Raman confocal spectroscopy. *Appl Spectrosc Rev*. 2020;55:158-171. doi:10.1080/05704928.2018.1558232



58. Leveen HH, Falk G, Borek B, et al. Chemical acidification of wounds. An adjuvant to healing and the unfavorable action of alkalinity and ammonia. *Ann Surg.* 1973;178:745-753. doi:[10.1097/0000658-197312000-00011](https://doi.org/10.1097/0000658-197312000-00011)
59. Hulst AC, Hens HJH, Buitelaar RM, Tramper J. Determination of the effective diffusion coefficient of oxygen in gel materials in relation to gel concentration. *Biotechnol Techn.* 1989;3:199-204.
60. Colom A, Galgoczy R, Almendros I, Xaubet A, Farr R. Oxygen diffusion and consumption in extracellular matrix gels: implications for designing three-dimensional cultures. *J Biomed Mater Res A.* 2013;102:2776-2784. doi:[10.1002/jbm.a.34946](https://doi.org/10.1002/jbm.a.34946)
61. Gottrup F. Oxygen in wound healing and infection. *World J Surg.* 2004;28:312-315. doi:[10.1007/s00268-003-7398-5](https://doi.org/10.1007/s00268-003-7398-5)
62. Schreml S, Szeimies RM, Prantl L, Karrer S, Landthaler M, Babilas P. Oxygen in acute and chronic wound healing. *Br J Dermatol.* 2010;163:257-268. doi:[10.1111/j.1365-2133.2010.09804.x](https://doi.org/10.1111/j.1365-2133.2010.09804.x)
63. Gupta S, Laskar N, Kadouri DE. Evaluating the effect of oxygen concentrations on antibiotic sensitivity, growth, and biofilm formation of human pathogens. *Microbiol Insights.* 2016;9:MBI.S40767. doi:[10.4137/mbi.s40767](https://doi.org/10.4137/mbi.s40767)
64. Russell AD, Path FRC. Chlorhexidine: antibacterial action and bacterial resistance. *Infection.* 1986;14:212-215. doi:[10.1007/BF01644264](https://doi.org/10.1007/BF01644264)
65. Kadam S, Madhusoodhanan V, Dhekane R, et al. Milieu matters: an in vitro wound milieu to recapitulate key features of, and probe new insights into, mixed-species bacterial biofilms. *Biofilm.* 2021;3:100047. doi:[10.1016/j.biofilm.2021.100047](https://doi.org/10.1016/j.biofilm.2021.100047)

SUPPORTING INFORMATION

Additional supporting information can be found online in the Supporting Information section at the end of this article.

How to cite this article: Thaarup IC, Lichtenberg M, Nørgaard KTH, et al. A collagen-based layered chronic wound biofilm model for testing antimicrobial wound products. *Wound Rep Reg.* 2023;31(4):500-515. doi:[10.1111/wrr.13087](https://doi.org/10.1111/wrr.13087)